arXiv:astro-ph/9605137v1 22 May 1996

RED GIANT–DISK ENCOUNTERS: FOOD FOR QUASARS?

P.J. Armitage[1,2]

W.H. Zurek[2]

M.B. Davies[1]

ABSTRACT

We explore the role that red giants might play in the fuelling and evolution of Active Galactic Nuclei. Due to their large radii and the low binding energy of the stellar envelope, giants are vulnerable to envelope stripping from collisions with the accretion disk. Using hydrodynamic simulations we show that such collisions will typically deposit a substantial fraction of the envelope mass into the disk on each passage. Repeated encounters will then lead to the complete destruction of the star save for the dense core. We estimate the rate of fuel supply by this mechanism using simple models for the AGN disk and central stellar cluster. If the central stellar density is $\sim 10^7\ M_\odot\ \mathrm{pc}^{-3}$, then stripping of giants could account for the activity of typical AGN provided that the accretion disk extends out to ~ 0.1 pc. For AGN with smaller disks, or clusters of lower central density, giant stripping could supply gas enriched via stellar nucleosynthesis to a disk replenished from some other source. We find that, for typical parameters, this mechanism is able to supply important quantities of gas to the disk at lower stellar densities than previously proposed stellar fuelling models for AGN.

[1]Institute of Astronomy, Madingley Road, Cambridge, CB3 0HA, UK

[2]Theoretical Astrophysics, T-6, MS B288, LANL, Los Alamos, NM 87545, USA

1. INTRODUCTION

Understanding the origin and evolution of the fuel supply that feeds quasars and other Active Galactic Nuclei (AGN) is a key mystery in the astrophysics of these systems. To account for luminosities as high as $\sim 10^{46}$ erg/s the most efficient conceivable process - accretion onto a black hole - requires a mass supply of order one solar mass per year. That matter (which over the lifetime of the active phase may amount to 10^8 $M_\odot$ or more) must be transported from galactic scales down to the Schwarzschild radius of the hole at just a few A.U. Evidently this transport mandates an efficient mechanism for disposing of the inflowing material's angular momentum.

A partial solution to the problem is provided by invoking the presence of an accretion disk in the immediate vicinity of the hole. Although the details are uncertain, viscosity in the disk transports angular momentum outward, and thereby permits mass to flow inward. Recent observations by *ASCA* of relativistically–broadened iron $K\alpha$ lines lend strong support to the idea of the existence of both massive black holes and disks in AGN (Tanaka et al. 1995). For the purpose of fuelling the hole, however, the disk is unlikely to provide more than a short term reservoir of mass, as models suggest that the disk mass is only a small fraction (perhaps 10^{-3} for a $10^8 M_\odot$ black hole) of the mass of the hole (e.g. Clarke 1988). Even allowing for generous uncertainties in our models of accretion disks, therefore, it seems inevitable that the disk itself must be continually replenished from some further, external, source of mass.

Two possibilities suggest themselves for the source of this external fuel supply. In the first, the disk could be fed by gas funnelled in from large (kpc) galactic scales, perhaps as a consequence of interactions between the AGN host galaxy and its neighbours (Hernquist & Mihos 1995). This scenario is attractive insomuch as there is undoubtably sufficient mass in gas at those large scales, though whether it can be transported to the sub-parsec scales of the accretion disk efficiently and without forming stars in the process is less clear. As a second possibility, the disk could be resupplied as a consequence of interactions occurring in a dense nuclear star cluster. Such clusters are observed in many well-studied nearby galaxies, with the core of M32 exhibiting a central stellar density exceeding $10^7 M_\odot \mathrm{pc}^{-3}$ (Lauer et al 1992; Crane et al 1993). Clusters of similar or modestly greater ($\sim 10^8$ $M_\odot \mathrm{pc}^{-3}$) richness then have the potential to be a significant source of AGN fuel–*if* a mechanism exists that allows the AGN to tap into that supply.

Disruption of stars in the tidal field of the black hole was suggested by Hills (1975) as a possible way to liberate the gas. Disruption occurs when the pericentre $r_{\min}$ of the orbit becomes comparable or smaller than the 'tidal' radius

$$R_{\mathrm{T}} \simeq 5 \times 10^{12} \left(\frac{M}{10^6 M_\odot}\right)^{1/3} \left(\frac{R_*}{R_\odot}\right) \left(\frac{M_*}{M_\odot}\right)^{-1/3} \mathrm{cm} \qquad (1)$$

where M is the hole mass (Rees 1988). An attractive prediction of this scenario is that activity should turn off when the central black hole has grown to the point that R_{T} is comparable to the

Schwarzschild radius,

$$R_{\rm BH} = 2GM/c^2, \tag{2}$$

after which stars are swallowed whole without significant release of radiation. For solar type stars this occurs when the black hole has reached a mass of a few $\times 10^8\ M_\odot$.

For the purpose of long-term fuelling of the black hole, however, this mechanism proves inadequate. Rapid disruption of stars passing within $R_{\rm T}$ depletes a region in phase space which is refilled via relaxation of the stars in the central cluster on a timescale $\sim 10^8$ yr. This rate is insufficient to provide enough fuel for the most luminous AGN (Shields & Wheeler 1978).

Other possibilities that have been assayed include mass loss from stellar winds, which might be enhanced as a result of the AGN's ultraviolet or high energy particle flux. A generic problem with such ideas is that gas released throughout the volume of the nuclear star cluster is vulnerable to being expelled by the radiation pressure from the central source. If only a fraction of the liberated mass reaches the disk or black hole then the demands placed on the supply of mass are appropriately aggravated.

The interaction between a nuclear star cluster and the accretion flow has been explored for the case of main sequence stars by a number of authors. For such stars collisions with the disk will tend to expel matter out of the disk plane while leaving the star relatively unscathed. This mechanism has been proposed as an origin for the gas producing the broad emission lines seen in AGN spectra (Zurek, Siemiginowska & Colgate 1991, 1994; see addendum in ApJ XXXX). Repeated collisions will gradually dissipate the star's orbital energy and in time drag it bodily into the plane of the disk (Syer, Clarke & Rees 1991). The consequences of stars captured in this fashion, for example for the metallicity of quasar accretion disks, have been extensively investigated (Artymowicz 1993; Artymowicz, Lin & Wampler 1993).

Here, we extend previous studies on star-disk interactions to consider the case of giant stars, with radii typically $\sim 100 R_\odot$. The greatly increased geometric area and reduced binding energy suggest that such stars should be susceptible to large-scale stripping of mass on collision with the disk (Zurek, Siemiginowska & Colgate 1994). Within some critical radius $R_{\rm crit}$ collisions will then destroy the star and unbind the envelope mass within the red giant lifetime. The value of $R_{\rm crit}$ will depend on the extent and properties of the disk as well as the velocity and structure of the star, but as we show later it is invariably larger than the radius within which stars are trapped while still on the main sequence. If $R_{\rm crit}$ and the central stellar density are sufficiently large, this mechanism could then provide an important source of fuel for the central black hole.

The plan of this paper is as follows. In section 2 we discuss the numerical methods and initial conditions of our calculations. In section 3 we present results of hydrodynamic simulations of the star-disk interaction for a range of stellar velocities v_*, and disk surface densities Σ. Our aim is to delineate that portion of the $v_* - \Sigma$ parameter space in which collisions lead to significant envelope loss. In section 4 we then combine the results of our calculations with simple models for the accretion disk and stellar cluster, in order to estimate how much fuel could be provided to the

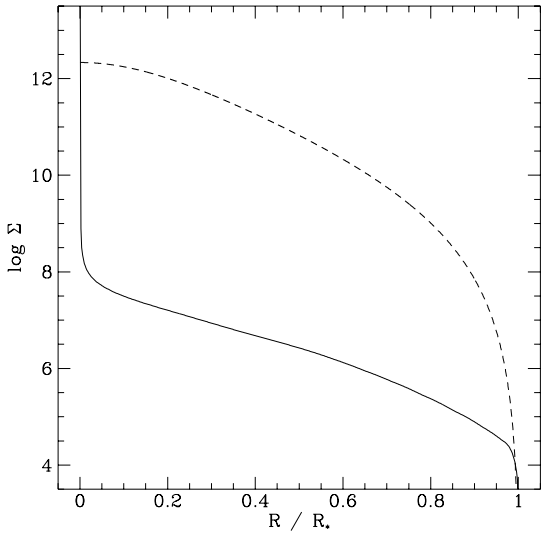

Fig. 1.— Log of the column density Σ (g/cm^2) as a function of the fractional stellar radius R/R_*. The solid line shows the profile for the red giant model used in the simulations; the dashed line represents the profile for an $n = 3$ polytrope of equal mass.

AGN by this mechanism. Section 5 summarises our results and conclusions.

2. NUMERICAL METHOD AND INITIAL CONDITIONS

The calculations described here were performed using a three-dimensional smoothed particle hydrodynamics code (SPH), minimally modified from that described by Benz (1990). This code has been extensively used in other simulations of stellar collisions (eg Davies, Benz & Hills 1991), and has been shown to give the same results on such problems as codes based on alternative numeric techniques (eg PPM–Davies et al. 1993).

In constructing our model star, we commence with a red giant structure calculated using the latest version of the Eggleton stellar evolution code (Pols et al. 1995 and references therein). The model is computed for a mass of $1M_\odot$, with a core mass of $0.45M_\odot$ and a radius $R_* \simeq 150R_\odot$. We take this model as being reasonably representative of red giant structures in galactic nuclei, while acknowledging that a more complete investigation than is attempted here should consider a range of stellar masses and radii. The model also ignores the possible consequences of the star's proximity to the AGN, though we note at this stage that the main effect of irradiation on giants is to *increase* their radii (Tout et al. 1989), which would tend to accentuate envelope loss on collision with the disk.

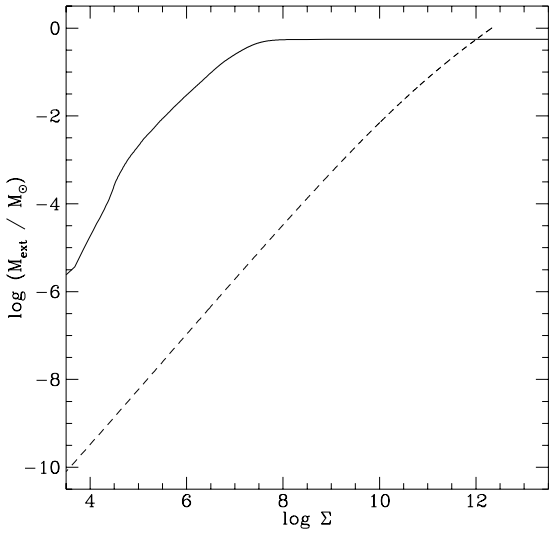

Fig. 2.— Integrated stellar mass exterior to a cylindrical radius with given column density Σ. The solid line shows the profile for the red giant model used in the simulations; the dashed line represents the profile for an $n = 3$ polytrope of equal mass.

The structure of the giant model is shown in Fig. 1, which plots the column density through the star ($\Sigma_* = \int \rho_* \mathrm{d}z$) as a function of the fractional radius R/R_*. For comparison we also show the structure of a main sequence star of the same mass, modelled as an $n = 3$ polytrope. For the red giant the typical column densities near the outer edge of the envelope are comparable to those seen in models of AGN accretion disks ($\Sigma \sim 10^4 - 10^5$ gcm^{-2}), while for the main sequence star the densities are several orders of magnitude greater. Thus if each collision strips off an annulus of mass with column density below some critical threshold (and we show later that this is indeed a reasonable estimate), then the red giant is vastly more susceptible to mass loss. This is quantified in Fig. 2, which plots the mass exterior to a given column density for the two models. At the relatively low Σ values found in AGN disks, the giant has a vulnerable mass fraction more than four orders of magnitude in excess of a main sequence star of the same mass. This implies that a star may survive repeated disk transits on the main sequence yet be destroyed relatively swiftly on reaching the red giant phase of its evolution.

To represent the stellar structure in SPH, we replace the core of the giant with a single point mass that interacts with the remaining particles via gravitational forces only. The envelope is modelled using 2274 SPH particles that are set down on a close-packed grid with masses proportional to the local density in the model star. As the density in an SPH calculation is not a local quantity this is a crude procedure, but it gives a density run that matches the stellar model to about 20% over 2 orders of magnitude in density (Fig. 3), which is is adequate for our purposes here. The internal energy and pressure of the particles are then set to ensure hydrostatic

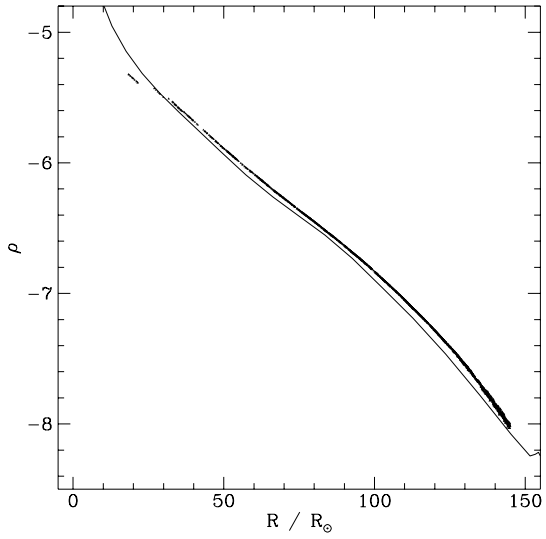

Fig. 3.— Log of the stellar density ρ/gcm^{-3} for the red giant used in our simulations as a function of radius. Solid line is the output of the stellar model, the symbols depict ρ at the positions of the particles in the SPH realisation.

equilibrium, using an equation of state that includes a mixture of gas and radiation pressure,

$$P = \frac{\rho \mathcal{R} T}{\mu} + \frac{\alpha T^4}{3}, \tag{3}$$

where $\mu = 0.6$ is the mean molecular weight and α the radiation constant. We have verified that stars modelled using this procedure are stable for at least several sound crossing times, which is an order of magnitude longer than the duration of the star-disk simulations.

For the disk we adopt a simple approach. The timescale for the star to transit the disk is only $\sim 10^6$ s, which is negligible compared to any timescale in the disk. We therefore represent the disk as a column of initially cold gas, with a gaussian density profile in the vertical direction (corresponding to an isothermal temperature distribution). Disk models suggest that the thickness of the disk is at least an order of magnitude greater than the size of even our giant star, so we pick a scale height H such that the density gradient across the star is small. For our main simulations we take $H = 600 R_\odot$, and truncate the disk in the vertical direction at 1.5 scale heights. We also experiment with other choices for H. With these parameters, we achieve comparable resolution in the star and disk with around 19,000 disk particles.

3. RESULTS

Table 1 lists the main parameters for the SPH simulations of star-disk encounters, the stellar velocity v_*, disk surface density Σ, and scale height H. We also tabulate the impacting disk mass $M_i = \pi R_*^2 \Sigma$, the incident momentum p_i, and kinetic energy E_i. As the binding energy of the model stellar envelope is only 1.6×10^{46} erg, *all* of these collisions have the potential in principle to unbind a large fraction of the stellar material. The final column in the table shows the main result of these calculations–the mass loss from the red giant–evaluated at a time 0.5 disk transit times after the star exits the disk. For all except the most violent collisions (which have anyway almost totally destroyed the stellar envelope by this stage) the induced mass loss has ceased by this time.

Figure 4 (*omitted from this draft*) shows a montage of frames from simulation E, where at each snapshot we have plotted particles within 2 SPH smoothing lengths of the $y = 0$ plane. This is the most energetic encounter, and as such demonstrates most clearly the two effects leading to mass loss. Firstly, momentum transfer between the disk gas and the star can bodily strip material from the sides of the star. This reduces the cross-sectional area the star presents to the disk, and creates a wake composed primarily of stellar material behind the star. Second, the disk gas impinging on the front surface of the star shock heats and compresses the material there. When the star emerges from the disk the heated gas then blows off as an almost spherical expanding cloud. These general hydrodynamic properties of the collision are very similar to those seen in simulations of stars impacted by shells of supernova ejecta (Fryxell & Arnett 1981; Taam & Fryxell 1984; Livne, Tuchman & Wheeler 1992). For supernovae that explode with red giant companions, indeed, the energy and momentum of the encounter are similar to those considered here. The main difference is then the relative thickness of the disk compared to the star–unlike shells of supernova ejecta typical AGN disks are always many stellar radii thick.

3.1. Mass loss

Figure 5 shows for runs A-E the bound mass in the stellar envelope as the star crosses the disk. We compute the bound mass at regular intervals by summing the masses of particles whose total energy (gravitational plus internal and kinetic) is less than zero. These simulations all have the same disk surface density (10^5 gcm^{-2}) and scale height ($H = 600 R_\odot$), and differ only in the stellar velocity. To facilitate comparison between the runs, we scale the time axis so that the disk crossing takes place between (in arbitrary time units) $t = 10$ and $t = 110$ for all the simulations.

From the figure, it can be seen that the behaviour divides into two regimes. The two most energetic collisions (D and E) disrupt the stellar structure entirely. Mass loss during the disk crossing is rapid, and most of the gas in the remnant that emerges from the disk is itself formally unbound from the white dwarf core. This prompt destruction of the star as a consequence of a

Fig. 4.— Omitted from this draft due to size

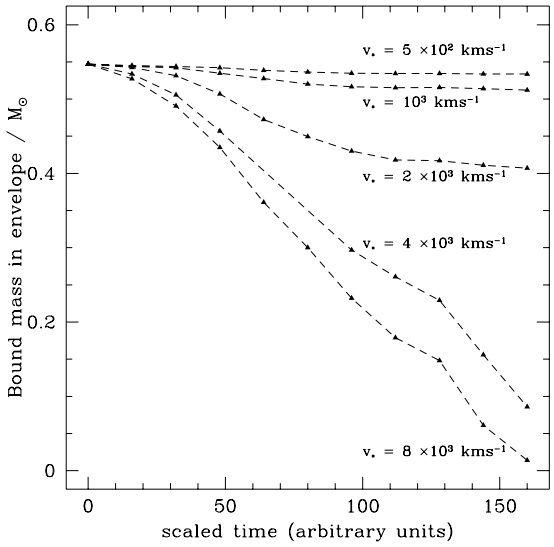

Fig. 5.— Bound mass in the stellar envelope as the star passes through the disk is shown here for runs with different impact velocities. The time axis has been scaled so that for each simulation the disk transit time is constant at 100 units. From top to bottom, the impact velocities were $v_* = 500$ km/s, 1000 km/s, 2000 km/s, 4000 km/s and 8000 km/s. For each case the disk surface density was 10^5 gcm^{-2}.

single disk passage occurs at this disk surface density for velocities of around 4000 km/s or greater. For AGN, that implies radii in the disk of less than 6000 R_{BH}, which as we shall show in Section 4.2 encompasses all the non-self-gravitating disk in a supermassive system of 10^8 $M_\odot$.

Less violent impacts (A-C) produce smaller fractions of stripped and ablated mass, and leave the inner regions of the star relatively unaffected. In these cases the rate of mass loss declines rapidly once the star has exited the disc, and so the final bound mass in our simulations is likely to give a good estimate of the total mass loss from the disk encounter. We find mass loss that ranges from 0.14 $M_\odot$ for the $v_* = 2000$ km/s run down to approximately 1% of a solar mass for the $v_* = 500$ km/s simulation.

3.2. Comparison with analytic predictions

To further interpret our simulations, we compare our numerical results to the semi-analytic theory developed by Wheeler, Lecar & McKee (1975, henceforth WLM) for the analogous situation of a star impacted by a supernova blast wave. Although we have already noted that there are important differences between that scenario and the star-disk encounter, the WLM theory has the

merit of providing a simple baseline against which to compare results. In the case of supernovae the theory has been shown to agree closely with detailed calculations (Fryxell & Arnett 1981).

Following WLM, we identify two components to the total mass loss. First, direct momentum transfer strips matter from the outside of the star down to some fraction of the stellar radius x_{crit}. This critical radius is that where the momentum transfered to a cylindrical shell is just sufficient to accelerate it to the stellar escape velocity $v_{\rm es}$ at that radius. As the impacts we are considering are highly supersonic ($v_* \gg v_{\rm es}$) this condition implies that mass is lost exterior to the cylinder where

$$\Sigma_*(R) = \left(\frac{v_*}{v_{\rm es}(R)}\right)\Sigma. \tag{4}$$

The quantity $\Sigma_*(R)$ is the column density through the star as plotted in Fig. 1. The stripped mass fraction by this direct mechanism, $F_{\rm strip}$, is then the total mass in the envelope exterior to a cylinder of radius $R_* x_{crit}$. From our red giant model $x_{\rm crit}$ and hence $F_{\rm strip}$ are straightforward to evaluate for a given incident momentum p_i.

Calculating the second, ablation component of the mass loss requires computing the heating generated by the shock that is driven into the star as a consequence of the collision. As the star exits the ejecta shell or disk, this thermal energy will become available as kinetic energy as the heated material 'boils off' the stellar surface. WLM give the result,

$$F_{\rm ablate} \approx \Psi x_{\rm crit}^2, \tag{5}$$

where their parameter Ψ is given in our notation by,

$$\Psi = M_i\left(\frac{v_*}{v_{\rm es}} - 1\right). \tag{6}$$

For highly supersonic encounters, Ψ is thus a measure of the incident momentum.

Figure 6 compares the WLM predictions with our numerically derived mass loss estimates for runs A–E. At high velocities of 4000 km/s or greater there is reasonable agreement between the mass loss seen in our simulations and the total predicted by the WLM analysis $F_{\rm total} = F_{\rm strip} + F_{\rm ablate}$. Both agree that at these velocities essentially all of the stellar envelope becomes unbound as a consequence of the collision.

At lower impact energies and momenta, we find that $F_{\rm strip}$ alone provides a good estimate of the mass loss seen in the simulations, suggesting that for these lower velocity ($v_* \leq 1000\ km/s$) encounters mass loss is driven primarily by momentum transfer rather than ablation. This transition as the velocity decreases is plausible on physical grounds–the large thickness of the disk relative to the stellar radius means that the collision is less like a single impulsive impact and more closely resembles a steady flow, albeit one in which the star undergoes steady stripping. Thus compared to the supernova case the strength of shock heating and ablation is liable to be reduced, leaving the directly stripped component dominant at low velocity. In support of this interpretation we note that repeating run C with the disk scale height halved (run I) leads to a doubling of the

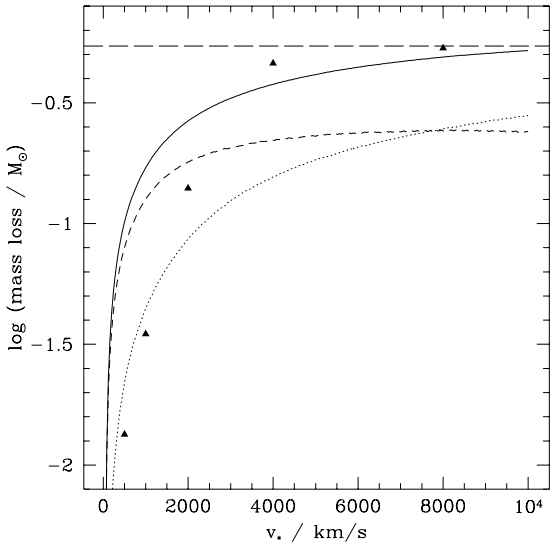

Fig. 6.— Stellar envelope mass loss as a function of encounter velocity. The symbols show the results of SPH simulations, the lines represent the expected mass loss using the WLM approximation (see text). Dotted line is $F_{\rm strip}$, dashed line is $F_{\rm ablated}$, and the solid line the total mass loss predicted. The dashed horizontal line represents total loss of the stellar envelope.

mass loss. Whereas run C shows mass loss intermediate between $F_{\rm strip}$ and $F_{\rm total}$, run I exhibits mass loss given closely by $F_{\rm total}$. Table 2 shows the results for all the runs described here.

From our simulations we can then identify two regimes. For high velocities and/or small disk scale heights the mass loss is large and can be approximated well by the total mass loss predicted by WLM, $F_{\rm total}$. This result agrees with the supernova studies referred to above. Conversely for lower velocity encounters with disks that are thick compared to the stellar size the mass loss is substantially reduced below the WLM prediction. In this case we can take $F_{\rm strip}$ alone as a reasonable estimate of the mass loss that will occur in the collision.

3.3. Post-encounter stellar structure

For the purpose of supplying fuel to the disk, the most important collisions are those that occur at relatively low velocity at a large radius in the disk. Although the mass loss per collision is small, the cumulative effect of many such impacts dwarfs that of the violent impacts that unbind the envelope in a single disk transit. We quantify this statement in the following Section, but note here that it is only true if the equilibrium structure of the perturbed star is *at least* as vulnerable to stripping as the original model. If this is the case we can regard the mass loss predicted for a

given v_* and Σ by our simulations as a *lower* limit on the mass loss in subsequent disk encounters.

To calculate the post-encounter stellar structure we first note that radiation pressure is negligible in the bound stellar envelope of the remnant, so that the polytropic exponent γ is everywhere close to 5/3. From our SPH simulations we can then extract the polytropic constant K at the location of each particle,

$$K = \frac{P}{\rho^\gamma}. \tag{7}$$

Following the impact K displays considerable scatter as a function of radius. This is a result of the non-symmetric injection of entropy from the shock-heating of the envelope. We therefore average over angles to obtain a smooth approximation to $K(R)$ for use in calculating the structure. We also compute the mass interior to radius R to express K as a function of enclosed mass m. Physically we expect the star to settle to a new equilibrium with a spherically symmetric K distribution on of order the convective timescale–much shorter than the interval between collisions with the disk. Provided that this is the case our averaging procedure and assumption of spherical symmetry should be valid.

Combining the equation representing hydrostatic equilibrium,

$$\frac{\mathrm{d}P}{\mathrm{d}R} = -\frac{Gm\rho}{R^2}, \tag{8}$$

with equation (7) above then gives an expression for the stable density gradient in terms of the function $K(m)$,

$$\frac{\mathrm{d}\rho}{\mathrm{d}R} = -\frac{Gm\rho^{2-\gamma}}{\gamma K(m) R^2}. \tag{9}$$

This equation together with the known total mass of the remnant constitute an eigenvalue problem for the central density, which we solve using a shooting method to yield the equilibrium density profile.

The results of this analysis are shown in Fig. 7(a) for run A–the lowest velocity encounter considered here. The density profile of the inner regions ($R < 100\ R_\odot$) is predicted to be almost unaltered by the impact, as expected since the influence of the collision on the star is confined to the outer layers for the less violent impacts. The main effect of the increased entropy generated by the encounter is to puff–up the outer envelope, leading to an increase in the radius of about 30%.

Fig. 7 illustrates how the recomputed stellar model differs from the initial red giant in its vulnerable mass fraction, expressed as the mass $M_{\rm ext}$ exterior to a cylinder of column density Σ (cf Fig. 2). The post-encounter star is *more* vulnerable to stripping than the initial model, by factors of around 2 for the typical values of column density considered here. We are therefore confident that repeated star–disk encounters will act cumulatively to disrupt the stellar envelope, and regard the estimates given in Section 4 (where we assume that the total mass loss is linear in the number of impacts) as conservative predictions of the rate at which destruction occurs.

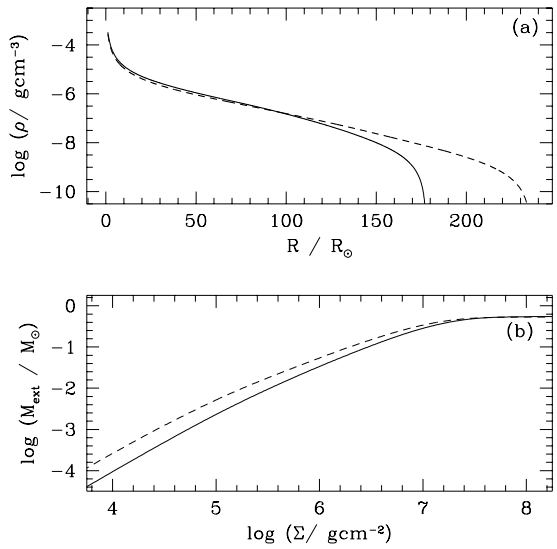

Fig. 7.— Equilibrium stellar structure calculated from the entropy profile of the red giant before (solid line) and after (dashed line) the encounter with the disk (run A). The upper panel shows the density profile, the lower panel the amount of mass exterior to a given column density as in Fig. 2.

4. IMPLICATIONS FOR THE FUELLING OF AGN

In the previous section we computed the mass stripping associated with a variety of star-disk collision parameters. The most violent collisions ($v_* \geq 4000$ km/s, $\Sigma = 10^5$ gcm^{-2}) lead to essentially complete stripping of the stellar envelope on a single disk transit. For less violent encounters the mass loss and disruption of the stellar structure is greatly reduced. In this regime we have used our results to validate a simple estimation procedure for the mass loss, based on the amount of momentum imparted to the stellar envelope by the impact.

In this Section we utilise the above results to investigate the significance of this mechanism for the fuelling of AGN. In Section 4.1 we calculate the radius out to which a disk could strip stars of their envelopes within the giant lifetime–this determines the volume of the cluster that is vulnerable to disk stripping. We compare this to the radii at which the competing processes of tidal disruptions; star-star collisions; and stellar trapping would operate. In Section 4.2 we calculate thin disk models to determine the 'target area' of the disk which has surface density sufficient to cause stripping. Finally in Section 4.3 we estimate the total mass that this mechanism might provide to fuel AGN activity for a variety of central stellar densities, and use the results of stellar evolution calculations to predict the evolution of the mass supply with time.

4.1. Determining the critical radii in the disk

On each disk transit, the star will be stripped down to a column density Σ_* given by equation (4). The corresponding mass loss can be directly read off from Fig. 2, which is well approximated for small $M_{\rm loss}$ by

$$M_{\rm loss} \sim \frac{v_*}{v_{\rm es}} \left(\frac{\Sigma}{10^4 {\rm gcm}^{-2}} \right) \times 10^{-5}\ M_\odot. \tag{10}$$

The timescale between encounters for stars orbiting at a radius R is

$$t_{\rm orbit} \approx \pi \sqrt{\frac{R^3}{GM}}, \tag{11}$$

where $M = M_{\rm BH} + M_{\rm c}$ is the total enclosed mass at that radius including the contribution from the cluster itself. Imposing the condition that at $R_{\rm crit}$ the star will just be stripped during the red giant lifetime $t_{\rm rg}$ then yields,

$$R_{\rm crit} \sim 0.05\ {\rm pc} \times \left(\frac{M}{10^6 M_\odot} \right)^{1/2} \left(\frac{t_{\rm rg}}{10^7 {\rm yr}} \right)^{1/2} \left(\frac{\Sigma}{10^4 {\rm gcm}^{-2}} \right)^{1/2} \left(\frac{v_{\rm es}}{50 {\rm kms}^{-1}} \right)^{-1/2}, \tag{12}$$

where we have inserted reasonable values for all the parameters. A $10^8\ M_\odot$ black hole is therefore capable of stripping red giants out to a distance of several tenths of a parsec, *if* the disk matter itself extends to that radius.

The red giant stripping process discussed here will evidently be important only if stars survive to become giants without first being destroyed by other processes, such as tidal disruption, stellar trapping, or star–star collisions. The radius at which stars are disrupted by the tidal field of the black hole is given by equation (1); we now estimate the critical radii for the other two competing processes.

In evaluating the timescale for stars to be ground into the plane of the disk we follow closely the approach of Syer, Clarke & Rees (1991). If the only mechanism leading to decay of the orbit is direct hydrodynamic drag on passing through the disk, then to order of magnitude the trapping timescale will be the time required for the star to impact its own mass of disk material. If on each passage the star collides with a mass $\Delta m = \pi R_*^2 \Sigma$,

$$t_{\rm trap} = \chi \frac{m_*}{\Delta m} t_{\rm orbit}, \tag{13}$$

where $\chi \sim 5$ is a dimensionless scaling factor that depends on the initial orbital parameters (Syer, Clarke & Rees 1991). Stars will be brought into the disk plane provided that $t_{\rm trap}$ is shorter than the relaxation time $t_{\rm relax}$, after which stars will typically have diffused onto less radial orbits. This criteria gives a radius interior to which stars will be trapped,

$$R_{\rm trap} \sim 10^{-3}\ {\rm pc} \times \left(\frac{M}{10^6 M_\odot} \right)^{1/3} \left(\frac{t_{\rm relax}}{10^8 {\rm yr}} \right)^{2/3} \left(\frac{R_*}{R_\odot} \right)^{4/3} \left(\frac{\Sigma}{10^4 {\rm gcm}^{-2}} \right)^{2/3} \left(\frac{m_*}{M_\odot} \right)^{-2/3}, \tag{14}$$

which is typically intermediate between the tidal disruption and giant stripping radii.

For the dense stellar systems we are considering, physical collisions may destroy stars before they even reach the giant stage of their evolution. We note at this stage that physical collisions might themselves be important in fuelling AGN, however they are undoubtably a different type of mechanism to that considered here and require detailed study to determine, for example, the efficiency of mass loss. For stars of a single representative radius R_*, a simple expression for the collision rate Γ is,

$$\Gamma = \pi R_*^2 v_* n(R), \tag{15}$$

where $n(R)$ gives the run of the stellar number density with radius. For simplicity, we assume a stellar profile that is a power-law in radius, with a stellar number density $n(R) = n_0 R^q$. For an isothermal sphere $q = -2$, while more detailed cusp solutions for stellar clusters containing a central black hole have $q = -7/4$ (Binney & Tremaine 1987 and references therein). A condition for collisions to be important at a radius R is that $\Gamma(R)\tau_{MS} \simeq 1$–in which case stars within that radius will be destroyed before completing their main sequence life τ_{MS}. For $q = -2$ this radius is

$$R_{\rm col} \sim 10^{-2}\ {\rm pc} \times \left(\frac{\tau_{MS}}{10^8 {\rm yr}}\right)^{2/5} \left(\frac{\overline{m}}{M_\odot}\right)^{-2/5} \left(\frac{M_c}{10^7 M_\odot}\right)^{2/5} \left(\frac{M}{10^6 M_\odot}\right)^{1/5} \left(\frac{R_*}{R_\odot}\right)^{4/5}, \tag{16}$$

where $\overline{m}$ is the mean stellar mass, M_c is the cluster mass enclosed within a radius of 1 pc, and M is the total mass within radius R.

Fig. 8 shows these radii as a function of black hole mass. For this plot we have taken parameters $t_{\rm rg} = 10^7$ yr, $t_{\rm relax} = 10^8$ yr, and $\tau_{MS} = 10^8$ yr. We assume a cluster with a mass $M_c = 10^7\ M_\odot$ within 1 pc, and a disk with a surface density Σ of 10^4 gcm^{-2} (ignoring for now the complication of having Σ itself a function of radius). There is a large parameter space here, but from the figure it is evident that the red giant stripping radius $R_{\rm crit}$ exceeds the other radii plotted by at least an order of magnitude for all black hole masses in the illustrated range. This implies, in particular, that most stars that are vulnerable to stripping as giants *will* survive to reach the red giant phase without suffering prior destruction by physical collisions. We note here that our estimate for the collision time on the main sequence is consistent with that of Begelman & Sikora (1991), who concluded that models in which red giants generated Broad Emission Lines from their stellar winds could be ruled out, because the stars would collide before reaching the giant phase. The apparent difference with our result is caused by the requirement for such models, (in which the stellar line-producing envelopes must provide a covering fraction towards the central source of ~ 0.1), to invoke a vastly greater stellar density in red giants than is required here.

Experimentation with the simple models presented above shows that, for most values of the parameters, we obtain plots qualitatively similar to Fig. 8, except that for lower central stellar densities the collision radius is reduced and lies interior to the trapping radius. We therefore conclude that for a disk that extends to large radius stellar stripping of giants will provide a greater source of fuel to the disk than the other stellar mechanisms considered here.

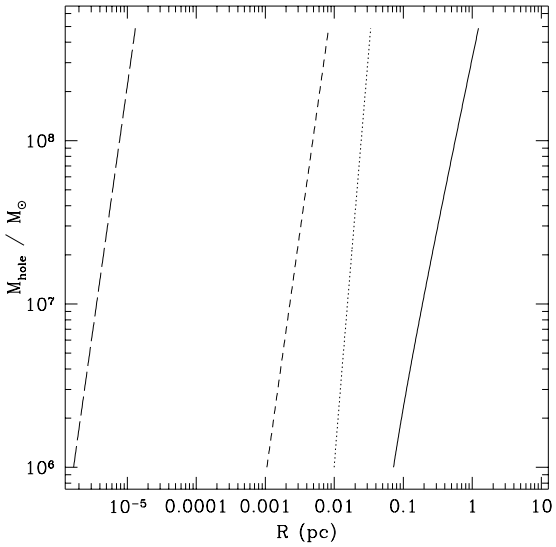

Fig. 8.— Radii at which various stellar fueling mechanisms become important for different masses of black hole. From left to right; tidal disruption (long dashes), stellar trapping (short dashes), star–star collisions (dots) and giant stripping (solid). This plot shows radii calculated for a cluster with $M_c = 10^7\ M_\odot$, with a disk of $\Sigma = 10^4$ gcm^{-2} extending to large radius.

4.2. Determining the target area of the disk

To determine the typical extent and properties of AGN accretion disks, we need the run of surface density with radius in the disk. To calculate this, we follow the approach of Clarke (1988) to construct vertically averaged thin disk solutions, which give the radial dependence of the surface density, sound speed, and other disk quantities. Although it is possible to go beyond vertically averaged models by solving for the details of the disk vertical structure, such calculations are more 'accurate' only if the site of energy dissipation in the disk is known. As this in turn depends on the unknown processes generating the viscosity, we cannot in practice expect to do better than the simple vertically averaged models presented here. Our models use the 'alpha-prescription' for the viscosity (Shakura & Sunyaev 1973); for completeness we set out the thin disk equation solved here in an Appendix.

Figure 9 shows contour plots of the disk surface density Σ as a function of radius and mass transfer rate $\dot{M}$ in the disk, for black hole masses that cover the range generally considered for AGN. These models assume constant $\dot{M}$ with radius, and an α of 0.1, similar to the inferred values in dwarf nova disk systems. The lower ($\sim 10^{-2}$) values favoured by some authors from analyses of UV variability (Siemiginowska & Czerny 1989) would increase the surface density in the disk, and thus somewhat enhance the efficacy of the stripping process. At each radius in our solutions, we

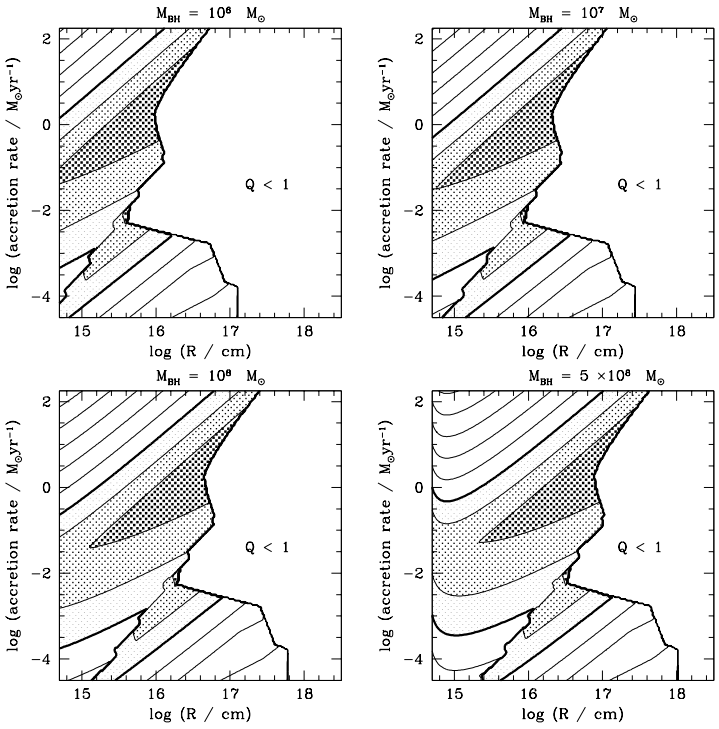

Fig. 9.— Contour plot of the disk surface density as a function of radius R and accretion rate through the disk $\dot{M}$. The panels depict different masses for the central black hole from 10^6 $M_\odot$ (top left), up to 5×10^8 $M_\odot$ (bottom right). Contours are plotted at intervals of 0.5 in $\log(\Sigma/\mathrm{gcm}^{-2})$, with the highest surface density regions shaded. The bold contour is at $\Sigma = 10^4 \mathrm{gcm}^{-2}$. The uncontoured region to the right of each plot is where the Toomre parameter, Q, is less than unity.

also evaluate the value of the Toomre Q parameter, which measures the importance of self-gravity,

$$Q = \frac{c_s \Omega}{\pi G \Sigma}. \tag{17}$$

In this equation c_s is the mid-plane sound speed and Ω the Keplerian angular velocity in the disk. If $Q < 1$ the disk becomes unstable to local gravitational instabilities, and although the structure in this regime is uncertain, the disk may develop spiral density waves or break up into clumps. As in such a situation the angular momentum is *not* transported via an α viscosity, consistency requires that we truncate our solutions when Q falls below unity.

Fig. 9 shows that for accretion rates between 10^{-3} and 10^1 $M_\odot$ yr^{-1} the surface density in the disk will be of order 10^4 gcm^{-2} or greater. This is the case for all the black hole masses considered here. However we also find that the disk would be expected to become self-gravitating at relatively small radii, ranging from $\sim 10^{16}$ cm (3×10^{-3} pc) for the 10^6 $M_\odot$ hole to around $\sim 10^{17}$ cm for the 10^8 $M_\odot$ case. The properties of the disk beyond these radii are unclear, though

calculations by Laughlin & Bodenheimer (1994) for self-gravitating protostellar disks suggest that gravitational torques transport angular momentum with an efficiency equivalent to an α of around 0.03. If this applies also to AGN disks, then it suggests that the average Σ in the self-gravitating regime should be at least as large as that calculated from the Shakura-Sunyaev analysis above.

4.3. Fuelling history

From Fig. 8 we find that supermassive black holes should be able to strip mass from red giants out to radii of ~ 0.1 pc provided only that their accretion disks extend to that radius. A 0.1 pc disk with average $\Sigma = 10^4$ gcm^{-2} has a mass of $\sim 10^6\ M_\odot$, which is still only a small fraction of the hole mass for the larger mass black holes. If the cluster mass $M_c = 10^7\ M_\odot$, then the mass of stars intersecting the disk will be of order $10^6\ M_\odot$, with the precise number dependent on the distribution of stellar orbits in the cluster (with more radial orbits leading to a greater fraction of vulnerable stars). If this mass of stars on orbits susceptible to stripping is fixed, then the rate at which this mass is liberated to the disk is controlled purely by stellar evolutionary processes. Once a given star reaches the red giant phase of its evolution its envelope mass will rapidly be deposited into the disk.

To investigate the evolution predicted by this model, we shall assume that the stellar population in the nuclear star cluster can be described as a coeval population with a power-law Initial Mass Function (IMF)

$$N(m) \propto m^{-\nu}. \tag{18}$$

Typically we take $\nu = 1.35$, corresponding to a Salpeter IMF, and impose a lower mass cut-off at the hydrogen-burning limit ($m \simeq 0.1 M_\odot$). If after a time τ (where $\tau = 0$ is the time of the initial star formation) stars of mass $m = m(\tau)$ are leaving the main sequence and becoming giants, then the rate at which mass is being deposited into the disk is

$$\dot{M} = \frac{\mathrm{d}N}{\mathrm{d}m}\frac{\mathrm{d}m}{\mathrm{d}\tau}\left(m(\tau) - m_{\rm core}\right). \tag{19}$$

In this expression $m_{\rm core}$ is the core mass which is not captured by the disk, while the envelope mass has been assumed to be instantaneously deposited into the disk once the star has evolved off the main sequence. This should be a reasonable approximation given that the red giant lifetime is much shorter than that on the main sequence.

Once the hydrogen burning stellar lifetime $\tau(m)$ is specified, equation (19) gives the mass deposition rate as a function of time. To gain some insight into the prediction of this model for the fuelling rate, we first assume that $\tau(m)$ is a power-law in the stellar mass. For masses of a few $M_\odot$, a crude estimate is,

$$\tau(m) \simeq 10^{10}\ \mathrm{yr}(m/M_\odot)^{-3}. \tag{20}$$

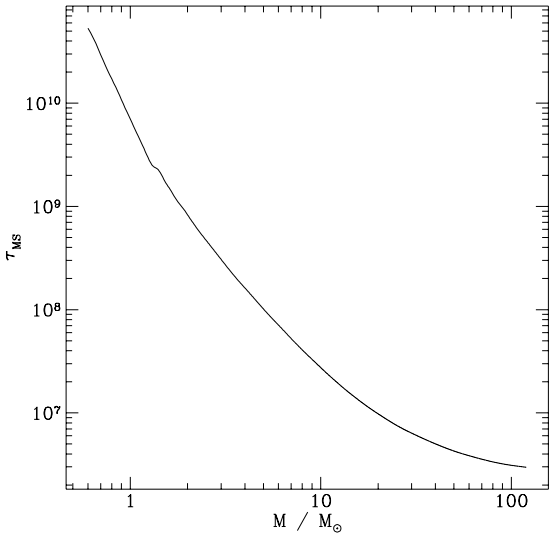

Fig. 10.— Main sequence lifetime as a function of stellar mass, from calculations by Fagotto et al. (1994).

At early times, when $m \gg m_{\rm core}$, the rate of deposition of AGN fuel is then given by

$$\dot{M} \sim \tau^{(\nu-4)/3} \sim \tau^{-0.9}, \tag{21}$$

where the final step uses for definiteness $\nu = 1.35$. The fuelling history is dominated by the steep dependence of the stellar lifetime on the mass, so that the mass deposition rate declines roughly inversely with time. If all other parameters of the system remained fixed (for example disk radius and surface density), we would then expect the supply of fuel today to be only a thousandth of the rate at an early (10^7 yr) epoch. Rapid evolution with cosmic time is, of course, a well-known property of AGN.

Figure 10 shows the results of detailed calculations of the hydrogen burning lifetime $\tau(m)$ by Fagotto et al. (1994), for stars in the mass range 0.6 $M_\odot < m <$ 120 $M_\odot$. These calculations assume a low metallicity ($Z = 0.004$) and employ modern (OPAL) opacities. Combining this function with an assumed IMF yields curves for the mass deposition rate, and the fraction of total mass liberated by a given time, that are shown in Fig. 11. Here we take $m_{\rm core} = 0.45\ M_\odot$, and vary the cluster mass and slope of the IMF.

For a cluster mass that intersects the disk of $10^7\ M_\odot$, we obtain a deposition rate at 10^7 yr of nearly $10^{-1}\ M_\odot {\rm yr}^{-1}$, which declines by approximately 2 orders of magnitude by 10^9 yr. For IMFs that are close to the Salpeter value, we find that about 20-30% of the initial cluster mass has been released to the disk within that time, though this is fairly sensitive to the assumed IMF. A steep IMF locks up a large fraction of the total mass in long-lived low-mass stars, and thus lowers the fraction of mass that reaches the giant phase and is supplied to the disk. We also note that the

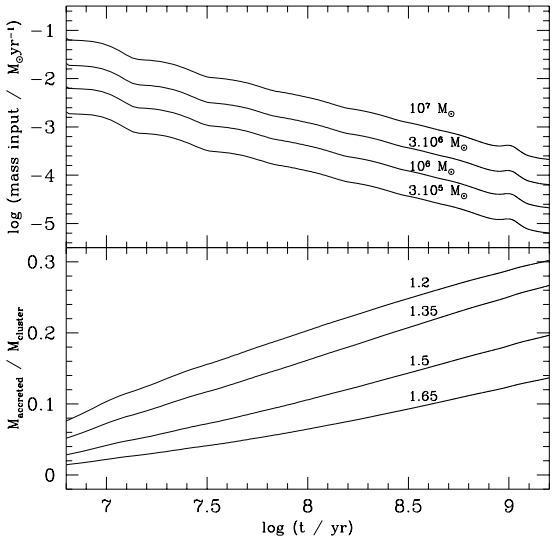

Fig. 11.— Upper panel: rate of mass deposition in the disk as a function of time assuming a constant disk surface density profile. The curves are plotted for different masses of stars on vulnerable orbits that intersect the disk, from top downwards $10^7\ M_\odot$, $3 \times 10^6\ M_\odot$, $10^6\ M_\odot$ and $3 \times 10^5\ M_\odot$. The lower panel shows the fraction of the stellar mass that has been stripped by a given time for various assumed IMFs, from top downwards we assume $\nu = 1.2$, 1.35, 1.5 and 1.65 respectively.

effect of an extended period of star formation would be to lower and 'smear out' the period of peak mass deposition. This would occur if the high mass star formation epoch exceeded approximately 10^7 yr.

Typical AGN luminosities are of the order of 10^{44} erg/s, which corresponds to an accretion rate of $\sim 10^{-2}\ M_\odot\ \mathrm{yr}^{-1}$ (assuming a 10% efficiency of converting rest mass into radiation). Fig. 11 then shows that mass deposition rates of this magnitude can be supplied from the early evolution of a cluster that has a few $\times 10^6 - 10^7\ M_\odot$ of stars on vulnerable, disk-intersecting orbits. For the accretion disk radii of ~ 0.1 pc postulated above, this requires a central stellar density within 1pc of the hole of order $10^7\ M_\odot$.

An immediate prediction of this model is that the rate of mass deposition into the disk should evolve rapidly. Fig. 11 is calculated assuming that the target area of the disk remains fixed, and so strictly represents the time-evolution of the mass supply if the disk is primarily replenished from some source other than star-disk collisions. In such a scenario, the main effect of the stripping would be to enrich the disk with the products of stellar nucleosynthesis. Such enrichment would be most significant at early times, shortly after the cluster was formed, and would subsequently drop off rapidly as shown in the Figure. Even faster evolution is predicted if star-disk collisions *dominate* the mass supply to the disk, as in this instance the radius to which the disk can strip stars would itself decrease with time. The evolutionary track would then move toward the lower

curves in the Figure, as fewer and fewer stars became vulnerable to destruction via disk impacts. Although the details would depend on the (poorly known) disk physics, the general scenario is then one in which a burst of star formation in the cluster leads to a short, (perhaps 10^8 yr, as by then the accretion rate would have fallen to the values where Σ starts dropping rapidly - Fig. 9), but intense flare in the AGN activity. As the mass deposition drops, so the disk weakens until it can no longer strip stars, and the activity then ceases altogether.

5. DISCUSSION

In this paper we have presented simulations of encounters of red giant stars with AGN accretion disks. We find that for encounters within around 0.1 pc of the black hole, and disk surface density exceeding 10^4 gcm^{-2}, the fractional mass loss on collision is sufficiently large that the star would not survive the red giant phase. Rather, the envelope mass would be deposited into the disk from the cumulative effect of numerous disk transits, leaving only a stripped core orbiting the black hole. The most violent collisions achieve this end in only a single passage. Although we have considered only one type of giant, we believe these conclusions are likely to apply equally to a range of red giant masses and structures.

We have compared the radius out to which red giants can be stripped via encounters with the disk with the radii at which stellar collisions and trapping by the disk become important. The stripping radius is generally one or two orders of magnitude greater than $R_{\rm col}$ and $R_{\rm trap}$, and indeed is most likely to be limited by the actual physical extent of the accretion disk. Even if the stellar density in the nucleus is relatively low, this mechanism could provide an important source of gas that has been enriched as a result of stellar nucleosynthesis. Artymowicz (1993) has suggested that heavy elements might be generated *in situ* by trapped stars accreting and then exploding as supernovae within the disk. The larger radius at which stripping can occur means that a similar quantity of enriched material could be provided to the disk by this process.

An immediate consequence of our models is that stars in the innermost regions of galaxies harbouring accretion disks will have their lifetime as red giants severely curtailed by star-disk collisions. The resultant modification of the stellar population is probably on too small a scale to be observable, though the depletion of the red giant population close to the black hole does cast further doubt on models that seek to invoke giants as important components in the central regions of AGN. Conversely, the rapid destruction of giants will *enhance* the rate of production of white dwarfs, which will remain as a dense cluster on disk-intersecting orbits. As suggested in a recent paper by Shields (1996), these single white dwarfs may accrete sufficient gas on passage through the disk to greatly enhance the rate of novae, and this provides yet a further mechanism for enriching the disk gas. We note that in principle better observations of the chemical mix in the centers of AGN could constrain which, if any, of these mechanisms – giant stripping, novae or supernovae – were important in supplying heavy elements to the gas.

How important might this mechanism be in fulfilling the *overall* fuelling requirements of quasars and other AGN? Since the stellar densities present in the cores of AGN remain unknown, it is impossible to answer this question with any great certainty. We find that typical AGN luminosities could be achieved from this mechanism if the central stellar densities are as high as $10^7\ M_\odot \mathrm{pc}^{-3}$ or greater, and the accretion disk extends to a few tenths of a pc. These are *lower* densities than are required for collisions between stars to liberate equivalent quantities of fuel. The activity of AGN powered by this fuel source would decline rapidly as the mass of stars becoming giants dropped, and would eventually switch off entirely as the disk became too tenuous to strip further stars. Such a scenario is not inconsistent with the evolutionary properties of quasars and AGN.

Although we have concentrated here on feeding the disk via a single population of stars in a central cluster, we also note that higher total masses of fuel could be provided by this mechanism if the depleted phase space could be replenished–perhaps by stars driven inward from the host galaxy by some means. This is of course essentially the 'interaction-driven' model of fuelling that we have previously mentioned. In such a scenario, the results given here imply that it is irrelevant whether the mass arrives at the nucleus in the form of gas or stars–even in the latter case a reasonable fraction of the total mass will be readily made available to feed the AGN activity.

Acknowledgements

We thank Jose Font-Roda, Chris Fryer and Cathie Clarke for commenting on earlier versions of this work, and Chris Tout for supplying the stellar model. PJA thanks T–6, LANL, for their hospitality over the summer. MBD acknowledges support from a Royal Society URF. This work was partially supported by IGGP, LANL.

APPENDIX: THIN DISK EQUATIONS

In Section 4.2 we have presented solutions to the vertically averaged thin disk equations. These are set out in, for example, Faulker, Lin & Papaloizou (1983), and follow the approach of Shakura & Sunyaev (1973). Explicitly we use the following forms. Local thermal equilibrium of an isolated annulus of the disk implies,

$$2\sigma T_e^4 = \frac{9}{4}\nu\Sigma\Omega^2, \tag{22}$$

where T_e is the disk effective temperature, σ the Stefan-Boltzmann constant, ν the kinematic viscosity, and Ω the Keplerian angular velocity. A vertically averaged treatment of the disk radiative transport gives a relation between the effective temperature and the central temperature T_c,

$$T_e^4 = \frac{8T_c^4}{3\kappa\Sigma} \tag{23}$$

where κ is the midplane opacity. The local mass flux $\dot{M}$ is

$$\nu\Sigma = \frac{\dot{M}}{3\pi}\left(1 - \sqrt{R_*/R}\right) \tag{24}$$

for a disk with a zero-torque ($\Sigma = 0$) inner boundary condition at a radius $R = R_*$. The alpha prescription for the viscosity is conventionally expressed as,

$$\nu = \frac{2}{3}\frac{\alpha P}{\Omega\rho} \tag{25}$$

with α a free parameter and ρ the central disk density. In lieu of greater knowledge of the form of the viscosity in AGN disks, we take α to be a constant, typically 0.1. The equation of state is as previously used,

$$P = \frac{\mathcal{R}\rho T_c}{\mu} + \frac{4\sigma}{3c}T_c^4. \tag{26}$$

Finally we have the equation representing hydrostatic equilibrium in the vertical direction,

$$H = \frac{\Sigma}{2\rho} = \frac{c_s}{\Omega} \tag{27}$$

where c_s is the midplane sound speed and H is the disk scale height.

The set of equations (22) - (27) can be readily solved once the opacity κ is specified. We utilise the analytic fits given by Bell & Lin (1994)–these are identical to those used by Lin & Papaloizou (1985) except for modifications to the low (below 3000K) temperature regime suggested by Alexander et al. (1989). Detailed expressions are as given in Bell & Lin (1994).

REFERENCES

Alexander, D.R., Augason, G.C., & Johnson, H.R., 1989, ApJ, 345, 1014

Artymowicz, P., 1993, PASP, 105, 691

Artymowicz, P., Lin, D.N.C., & Wampler, E.J., 1993, ApJ, 409, 592

Bell, K.R., & Lin, D.N.C., 1994, ApJ, 427, 987

Begelman, M.C., & Sikora, M., 1991, in AIP Conf. Proc. 254, Testing the AGN Paradigm, ed. S.S. Holt, S.G. Neff, & C.M. Urry (New York: AIP)

Benz, W., 1990, in The Numerical Modelling of Nonlinear Stellar Pulsations, ed. J.R. Buchler, Kluwer Academic Publishers, Dordrecht, p. 269

Binney, J., & Tremaine, S., 1987, Galactic Dynamics, Princeton University Press, Princeton, p. 545

Clarke, C.J., 1988, MNRAS, 235, 881

Crane, P., 1993, AJ, 106, 1371

Davies, M.B., Benz, W., & Hills, J.G., 1991, ApJ, 381, 449

Davies, M.B., Ruffert, M., Benz W., & Müller, E., A&A, 272, 430

Fagotto, F., Bressan, A., Bertelli, G., & Chiosi, C., 1994, A&AS, 105, 29

Faulkner, J., Lin, D.N.C., & Papaloizou, J., 1983, MNRAS, 205, 359

Fryxell, B.A., & Arnett, W.D., 1981, ApJ, 243, 994

Hernquist, L., & Mihos, J.C., 1995, ApJ, 448, 41

Hills, J.G., 1975, Nature, 254, 295

Lauer, T.R., et al., 1992, AJ, 104, 552

Laughlin, G., & Bodenheimer, P., 1994, ApJ, 436, 335

Lin, D.N.C., & Papaloizou, J., 1985, in Protostars and Planets II, eds. D.C. Black & M.S. Matthews, University of Arizona Press, Tucson, p. 981

Livne, E., Tuchman, Y., & Wheeler, J.C., 1992, ApJ, 399, 665

Pols, O., Tout, C.A., Eggleton, P.P., & Han, Z.W., MNRAS, 274, 964

Rees, M.J., 1988, Nature, 333, 523

Shakura ,N.I., & Sunyaev, R.A., 1973, A&A, 24, 337

Shields, G.A., 1996, ApJ, in press

Shields, G.A., & Wheeler, J.C., 1978, ApJ, 222, 667

Siemiginowska, A., & Czerny, B., 1989, 239, 289

Syer, D., Clarke, C.J., & Rees, M.J., 1991, MNRAS, 250, 505

Taam, R.E., & Fryxell, B.A., 1984, ApJ, 279, 166

Tanaka, Y., et al., 1995, Nature, 375, 659

Tout, C.A., Eggleton, P.P., Fabian, A.C., & Pringle, J.E., MNRAS, 238, 427

Wheeler, J.C., Lecar, M., & McKee, C.F., 1975, ApJ, 200, 145

Zurek, W.H., Siemiginowska, A., & Colgate, S.A., 1991, in AIP Conf. Proc. 254, Testing the AGN Paradigm, ed. S.S. Holt, S.G. Neff, & C.M. Urry (New York: AIP)

Zurek, W.H., Siemiginowska, A., & Colgate, S.A., 1994, ApJ, 434, 46; addendum ApJ, to appear Oct 10 issue

Table 1: RESULTS OF SPH STAR-DISK SIMULATIONS

Run	v_* (km/s)	Σ (g/cm^2)	H ($R_\odot$)	M_i ($M_\odot$)	p_i (gcm/s)	E_i (erg)	$M_{\rm loss}$ ($M_\odot$)
A	500	10^5	600	1.9×10^{-2}	1.9×10^{39}	4.7×10^{46}	1.3×10^{-2}
B	1000	10^5	600	1.9×10^{-2}	3.8×10^{39}	1.9×10^{47}	3.5×10^{-2}
C	2000	10^5	600	1.9×10^{-2}	7.5×10^{39}	7.5×10^{47}	1.4×10^{-1}
D	4000	10^5	600	1.9×10^{-2}	1.5×10^{40}	3.0×10^{48}	4.6×10^{-1}
E	8000	10^5	600	1.9×10^{-2}	3.0×10^{40}	1.2×10^{49}	5.3×10^{-1}
F	1000	10^4	600	1.9×10^{-3}	3.8×10^{38}	1.9×10^{46}	2.9×10^{-3}
G	4000	10^4	600	1.9×10^{-3}	1.5×10^{39}	3.0×10^{47}	5.8×10^{-2}
H	4000	2.5×10^4	600	4.7×10^{-3}	3.8×10^{39}	7.5×10^{47}	1.2×10^{-1}
I	2000	10^5	300	1.9×10^{-2}	7.5×10^{39}	7.5×10^{47}	2.6×10^{-1}

Table 2: COMPARISON WITH ANALYTIC ESTIMATES

Run	v_* (km/s)	Σ (g/cm^2)	H ($R_\odot$)	$M_{\rm loss}$ ($M_\odot$)	$F_{\rm strip}$ ($M_\odot$)	$F_{\rm wlm}$ ($M_\odot$)
A	500	10^5	600	1.3×10^{-2}	2.2×10^{-2}	1.0×10^{-1}
B	1000	10^5	600	3.5×10^{-2}	4.5×10^{-2}	1.7×10^{-1}
C	2000	10^5	600	0.14	8.6×10^{-2}	0.27
D	4000	10^5	600	0.46	0.16	0.38
E	8000	10^5	600	0.53	0.25	0.49
F	1000	10^4	600	2.9×10^{-3}	4.3×10^{-3}	3.0×10^{-2}
G	4000	10^4	600	5.8×10^{-2}	1.9×10^{-2}	9.1×10^{-2}
H	4000	2.5×10^4	600	0.12	4.7×10^{-2}	0.17
I	2000	10^5	300	0.26	8.6×10^{-2}	0.27